Volume 18, Number 2, 2025. pp. 141-155

Jordan Journal of Physics

ARTICLE

Calculation and Evaluation of the Best Orbit for Satellites Convenience to Transfer to the Geosynchronous Transfer Orbit (GTO)

Marwah Issa Abood Alnidawi and **Abdul-Rahman H. Saleh**

Departments of Astronomy and Space, College of Science, University of Baghdad, Baghdad, Iraq.

Doi: **https://doi.org/10.47011/18.2.4**

Received on: 14/10/2023; *Accepted on: 19/02/2024*

Abstract: This study focuses on optimizing satellite transfers from a low Earth orbit (LEO) to a geosynchronous transfer orbit (GTO) using Ariane 5 rockets. The primary objective is to select the best parking orbit, enhancing the mission stability and cost-effectiveness. Two key goals were identified: improving the initial conditions of parking orbits to reduce fuel consumption and evaluating perturbations affecting satellite trajectories during transfers. The methodology employs a dataset from Ariane 5-launched satellites utilizing MATLAB simulations and the Runge-Kutta method for accurate satellite position and velocity estimations under various perturbations. This research provides a detailed analysis of the propulsion and trajectory dynamics of five satellites, offering insights into orbital mechanics. The key findings include the significant impacts of atmospheric drag, solar radiation pressure, and gravitational effects on satellite trajectories. An inverse relationship was observed between the total velocity change and the fuel mass ratio, suggesting that lower velocity changes result in reduced fuel requirements, thereby improving launch vehicle efficiency and reducing costs. In conclusion, this study affirms the effectiveness of the Hohmann transfer method and underscores the importance of optimal parking orbit selection for successful GTO insertion. This lays the foundation for further research on satellite dynamics and orbital transfers, highlighting the need to manage orbital perturbations for reliable satellite missions.

Keywords: Satellite transfers, Geosynchronous transfer orbit, Hohmann transfer orbits, Ariane 5 rockets, Orbital mechanics, Perturbation analysis, Satellite trajectory.

1. Introduction

The deployment of satellites into the geosynchronous transfer orbit (GTO) is vital for a variety of space missions, encompassing global communications and Earth observation [1, 2]. This study focuses on optimizing satellite transfers from a low Earth orbit (LEO) to a GTO by employing widely used Hohmann transfer orbits [3, 4]. Our aim is to unravel the intricacies of these transfer processes, specifically utilizing the Ariane 5 rockets, renowned for their payload efficiency. This study focuses on the strategic selection of the optimal parking orbit, which is a crucial step that ensures mission stability and extensive coverage. The efficiency of this selection process not only streamlines satellite alignment with target orbits but also enhances the accuracy and cost-effectiveness of the mission [5, 6].

The Ariane 5 launch vehicle, with over 117 successful launches and a remarkable 96 percent success rate, serves as our primary focus [1, 5]. Its consistent performance in deploying satellites to various orbits, including the coveted GTO, has established it as a global benchmark, particularly for communications satellites [7, 8]. This research draws upon a range of studies investigating satellite perturbations, orbital elements, and transitions, thus providing a

Corresponding Author: Marwah Issa Abood Alnidawi **Email**: memaissa6@gmail.com

comprehensive backdrop for our study. Here is a chronological overview of these studies:

In 1993, Mains, conducted research on satellite trajectories, particularly concerning the transfer of satellites from Earth parking orbits. This study is detailed in the thesis titled "Transfer Trajectories from Earth Parking Orbits" [9]. In 2009, Al-Burmani and Aref investigated the impact of atmospheric drag and zonal harmonics on satellite orbits in low Earth orbit (LEO). Their findings emphasized the dominant role of atmospheric drag, resulting in a gradual decrease in orbit altitude over time [52].

In 2011, Wesam calculated satellite orbits while considering various perturbations, highlighting the significant influence of factors such as atmospheric drag and Earth's oblateness on LEO orbits [43]. In 2015, Almohammadi and Mutlag, made substantial contributions by modifying a model for calculating low Earth orbit trajectories [8].

In 2018, Wang and Zhang conducted a study investigating the impact of solar radiation pressure on changes in satellite orbits, providing valuable insights into this phenomenon [18]. Also in 2018, Yosif and Saleh carried out a comprehensive analysis of orbital maneuvers associated with the transition from low Earth orbit to geostationary Earth orbit [21]. Also in 2018, Kim and Lee conducted a thorough investigation into transfers between geosynchronous orbits, with a particular emphasis on the critical role played by atmospheric drag in such maneuvers [10].

In 2019, Chen *et al.* conducted a significant study on geosynchronous orbit transfers. Their research explored various factors affecting satellite paths during orbit transfers, with specific attention to perturbations in the process [16]. In the same year, Ibrahim and Saleh revisited Kepler's equation for elliptical orbits, presenting innovative solution methods and contributing to the advancement of this field [12].

In 2020, Farid, Abdul-Rahman, and Majeed explored methods for orbital transitions between two elliptical Earth orbits, emphasizing the importance of initial conditions and accounting for satellite mechanical anomalies [11]. Also in 2020, Rasha and Abdul-Rahman dedicated their research efforts to improving the accuracy of perturbed orbital elements for LEO satellites. Their work focused on enhancing the application of the fourth-order Runge–Kutta method [13]

This study is focused on the optimization of satellite transfers from low Earth orbit (LEO) to geosynchronous transfer orbit (GTO) through the utilization of Ariane 5 rockets. Particular emphasis is placed on selecting the optimal parking orbit and implementing MATLAB simulations, combined with the Runge-Kutta method, to estimate satellite positions and velocities under various perturbations.

A notable finding is the identification of an inverse relationship between total velocity change and the fuel mass ratio. This relationship suggests that minimizing velocity changes can enhance launch vehicle efficiency and reduce mission costs.

In comparison to prior research, this study distinguishes itself by its concentrated approach to parking orbit selection and its extensive utilization of numerical simulations, shedding light on a deeper understanding of satellite transfer processes. This research serves as a unique contribution to the field of satellite dynamics and orbital transfers.

2. Objective of the Study

This research is structured around two primary objectives. The first is to enhance the initial conditions of parking orbits, thereby reducing fuel consumption during transfer missions by ascertaining the efficacy of Hohmann transfer orbits from LEO to GTO. The second objective involves a thorough evaluation of the various perturbations affecting satellite trajectories during these transfers. This includes an examination of factors such as atmospheric drag, solar radiation pressure, gravitational effects, and magnetic field influences, all of which play pivotal roles in the trajectory of a satellite.

3. Data and Methodology

Our dataset comprises data archives from satellites launched via Ariane 5 rockets to the GTO [5]. These data, sourced from the official Ariane 5 website, form the empirical basis of this study. The methodology centers on the use of the parking orbit, which has been extensively documented in the context of the Hohmann transfer method, particularly in relation to co-axial elliptical orbits [14-16].

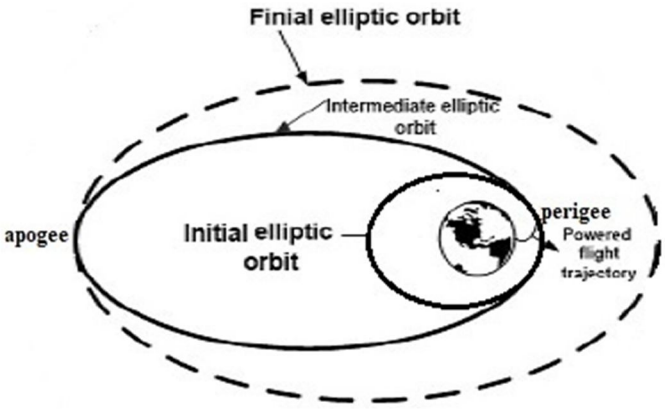

FIG. 1. Trajectory from parking orbit to geosynchronous transfer orbit (GTO) [14, 17].

To illustrate the concept of trajectory transfer from the parking orbit to the geosynchronous transfer orbit (GTO), Fig. 1 presents a visual representation. This figure depicts the path a satellite follows when transitioning from its initial parking orbit to its final GTO, showing the complexity and precision required in such maneuvers [18, 19].

Because celestial dynamics is a labyrinthine field, we implemented a MATLAB algorithm for an in-depth analysis of orbits from a heliocentric inertial reference frame (Appendix A). This code meticulously evaluates satellite movements, simulating the trajectory from the parking orbit to the GTO, as depicted in Fig. 1. Initial calculations focused on orbital elements in the absence of perturbation forces, followed by the inclusion of perturbing factors, such as Earth's oblateness, solar and lunar gravity, and solar radiation pressure. Utilizing the Runge-Kutta method allowed us to integrate motion equations, yielding precise estimations of the satellite positions and velocities at each step. This method is pivotal in determining the perturbed orbital elements, thereby delineating the satellite's ultimate trajectory (Appendix A).

3.1. Hohmann Transfers the Method between Coaxial Elliptical Orbits

The Hohmann transfer method is an efficient technique for transitioning spacecraft between two elliptical orbits, as shown in Fig. 2 [20]. This approach is instrumental in saving fuel and energy, thereby enhancing the cost-effectiveness and time-efficiency of space missions [21].

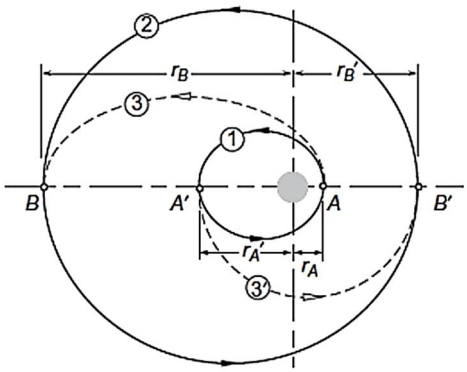

FIG. 2. Illustration of Hohmann Transfers between Coaxial Elliptical Orbits [20].

- Fundamental Equations:

The primary orbital parameter, represented by a, is the semi-major axis of an ellipse or the average satellite distance from the center of an elliptical orbit, calculated as

$$a = (r_p + r_a)/2 \quad (1)$$

where r_p and r_a are the perigee and apogee distances, respectively. This parameter is pivotal in determining the trajectory of a satellite [22].

- Velocity Calculations for Orbital Transitions:

To facilitate successful orbital transitions to GTO, we calculated the necessary velocity changes at different orbit stages [23]:

For initial orbit:

$$V_{p1} = \sqrt{\mu\left(\frac{2}{r_{p1}} - \frac{1}{a}\right)} \quad (2)$$

$$V_{a1} = \sqrt{\mu(\frac{2}{r_{a1}} - \frac{1}{a})} \quad (3)$$

For intermediate orbit:

$$V_{p2} = \sqrt{\mu(\frac{2}{r_{p2}} - \frac{1}{a})} \quad (4)$$

$$V_{a2} = \sqrt{\mu(\frac{2}{r_{a2}} - \frac{1}{a})} \quad (5)$$

For final orbit:

$$V_{p3} = \sqrt{\mu(\frac{2}{r_{p3}} - \frac{1}{a})} \quad (6)$$

$$V_{a3} = \sqrt{\mu(\frac{2}{r_{a3}} - \frac{1}{a})} \quad (7)$$

Here, V_p and V_a denote velocities at the perigee and apogee, respectively, and μ represents the standard gravitational parameter (μ: G Me = 398602.4415 at r in km) [23].

$$\Delta V1 = Vp2 - Vp1$$

$$\Delta V2 = Va3 - Va2 \quad (8)$$

$$\Delta Vtotal = \Delta V1 + \Delta V2$$

The total velocity change for orbital transfer (ΔVtotal) is the sum of the changes at the perigee (ΔV1) and apogee (ΔV2), as outlined in Eqs. (8)-(10). These calculations are critical for precise maneuvering and fuel efficiency [23].

- *Considerations for Launch Location:*

Launching from Kourou in French Guyana near the equator eliminates the need for inclination changes during the transfer. However, launches from other locations require calculating the rotational velocity change (ΔV_{rot}) to account for orbital inclination adjustments [24, 25]:

$$\Delta V_{rot} = \sqrt{{V_{a2}}^2 + {V_{a3}}^2 - 2{V_{a2}}^2{V_{a3}}^2\cos(\Delta i)} \quad (9)$$

where Δi is the orbital inclination change.

So:

$$\Delta V_{total} = \Delta V_1 + \Delta V_2 + \Delta V_{rot} \quad (10)$$

Equations (2)-(10) lay the groundwork for determining the essential velocities and changes required for effective orbital transfers, highlighting the importance of launch location and trajectory planning in space missions [26].

3.2. Satellite Motion Analysis under Perturbations:

Satellite motion in the presence of perturbations can be studied using two primary methods: special and general. This research utilizes Cowell's method, a specific type of special perturbation known for its simplicity and effectiveness. Cowell's method employs two first-order differential equations to analyze the trajectory of a satellite [27-29]:

$$\dot{\mathbf{r}} = \mathrm{v}$$

This equation represents the rate of change of the satellite's position vector, r, where v is the velocity vector [30].

$$\dot{\mathbf{v}} = -\frac{\mu}{r^3}\mathbf{r} + \mathbf{a_p} \quad (11)$$

Here, μ is Earth's gravitational constant, and a_p denotes the sum of perturbing accelerations affecting the satellite's orbit [31].

The perturbing accelerations (a_p) encompass several components [30, 31]:

$$\mathbf{a_p} = \mathbf{a_{J2}} + \mathbf{a_{drag}} + \mathbf{a_{SPR}} + \ddot{\boldsymbol{r}}_{\boldsymbol{l}} \quad (12)$$

where:

a_{J2}: geopotential acceleration due to Earth's oblateness,

a_{drag}: acceleration due to atmospheric drag,

a_{SPR}: solar radiation pressure acceleration, and

$\ddot{r}_l$: third-body gravity acceleration, representing the gravitational influence of celestial bodies other than Earth.

Equation (12) forms the core of our analysis, allowing us to understand the complex dynamics of the satellite motion under various perturbative forces. Detailed discussions and transactions of this method are thoroughly covered in the literature [6, 31].

3.2.1. Atmospheric Drag

The acceleration due to atmospheric drag (a_{drag}) is expressed as [32]:

$$\mathbf{a_{drag}} = -\frac{1}{2}\boldsymbol{\rho}\,\frac{\boldsymbol{C_D A}}{\boldsymbol{m}}\boldsymbol{v^2}\mathbf{i_v} \quad (13)$$

where ρ represents the atmospheric density, CD is the drag coefficient, A is the satellite's cross-sectional area perpendicular to the velocity vector, m is the mass of the satellite, v is the velocity of the satellite relative to the atmosphere, and iv is a unit vector in the direction of the satellite velocity. A negative sign

indicates that the acceleration direction is opposite to the velocity [33].

3.2.2. Non-spherical Gravitational Field of the Earth

The perturbative acceleration due to the Earth's non-spherical gravitational field is determined by factors including the Earth's radius (R_e) and the satellite's position components (x, y, z) [34-37]:

$$\mathbf{a}_{J_2} = \frac{-3\mu R_e^{\,2} J_2}{2r^7}\begin{bmatrix} x\left(x^2+y^2-4z^2\right) \\ y\left(x^2+y^2-4z^2\right) \\ z\left(3x^2+3y^2-2z^2\right) \end{bmatrix} \quad (14)$$

3.2.3. Third-Body Attractions

Third-body attractions refer to the gravitational impact of celestial bodies other than the Earth, such as the Moon. These forces lead to periodic and long-term fluctuations in various orbital elements. For instance, the gravitational influence of the Moon results in additional perturbations to the motion of the satellite [34, 38, 39].

$$\ddot{r} = -\frac{GM}{r^3}\vec{r} + GM_l\left(\frac{\vec{r}_{satl}}{{r_{satl}}^3} - \frac{\vec{r}_l}{{r_l}^3}\right) \quad (15)$$

The first term is due to the acceleration caused by Earth (central term). The additional perturbation acceleration caused by the gravitational attraction of the Moon acting on the satellite is then [40-43]:

$$\ddot{r}_l = GM_l\left(\frac{\vec{r}_l - \vec{r}}{|r_l - r|^3} - \frac{\vec{r}_l}{{r_l}^3}\right) \quad (16)$$

3.2.4. Solar Radiation Pressure Perturbation (SRP)

The acceleration from solar radiation pressure occurs when the Moon passes through a constellation; due to gravitational lensing and radiation from the constellation, more cosmic radiation is bent. This bent radiation impinges deep inside the atmosphere of the Earth, which produces more secondary gamma-radiation particles. For the Earth–to–GTO transfer, a_{SPR} is given by [44-47]:

$$a_{SPR} = \mu P_s C_R \frac{A}{m} \quad (17)$$

where C_R is the reflectivity coefficient, A is the satellite's cross-sectional area, m is the mass of the satellite, μ is a function of shadow (1 in full sunlight, 0 in umbra, and between 0-1 in penumbra), and P_s is the solar radiation pressure. The equation $(\frac{E}{C})$ accounts for the solar radiation constant E (1358 w/m²) and the speed of light in vacuum c [48-52].

4. Results and Discussion

In a comprehensive evaluation of the propulsion and trajectory parameters for five satellites launched by Ariane 5: NILESAT 201, JCSAT-12, ARABSAT 5A, WILDBLUE-1, and W3B (detailed in Tables 1 and 2), we discern the nuances of their journey from low Earth orbit (LEO) to geosynchronous transfer orbit (GTO). This transition, executed via the Hohmann transfer method, is a two-stage propulsion process that entails an initial velocity increase at the perigee (ΔV1) to extend the orbit and a subsequent burn at the apogee (ΔV2) to circularize at the GTO.

Table 1 shows the initial and final orbital elements for each satellite, such as the perigee and apogee altitudes, semi-major axis, eccentricity, and time for half an orbit (t = T/2). These figures indicate the energy requirements for transfer, with the semi-major axis and eccentricity dictating the orbit's size and shape, respectively, and consequently, the satellite's total orbital energy.

Table 2 sheds light on critical velocity parameters, such as perigee and apogee velocities pre- and post-burn, and the total required velocity change (ΔV_{Total}). The ΔV_{Total} is a direct indicator of the mission's propellant budget, with lower values signifying more fuel-efficient transfers, thereby impacting the economic and operational aspects of the mission.

The data suggest that the transfer efficiency of each satellite varies and is influenced by its mass, initial orbit, and specific perturbations encountered, such as gravitational variations, atmospheric drag, and solar radiation pressure. These perturbations require precise velocity adjustments to maintain the desired trajectory.

A key finding is the inverse relationship between the total velocity change (ΔV_{Total}) and fuel mass ratio (Δm/m1). A lower ΔV_{Total} corresponds to a reduced need for fuel, improved launch vehicle performance, and decreased launch costs. Such optimization is essential for mission success and hinges on the strategic planning of orbital transfer, considering the unique characteristics of each satellite and the trade-offs between velocity changes, fuel

consumption, and operational requirements in GTO.

Collectively, the insights from Tables 1 and 2 provide a scientific foundation for determining the preliminary conditions for future satellite launches. This integrated analysis enables the design and execution of fuel-efficient and cost-effective orbital maneuvers, ensuring that satellites are inserted into their intended orbits with adequate fuel reserves for their operational lifespans. Moreover, it sets a precedent for future mission planning and launch strategy refinement.

TABLE 1. The five most efficiently transferred satellites launched by Ariane 5 using the Hohmann transfer method between coaxial elliptical orbits.

	Flights	Perigee Altitude (km)	r Perigee (km)	apogee Altitude (km)	r apogee (km)	Semi-major axis (km)	Eccentricity (e)	Time (Sec)	t = T/2 (Sec)
1	The NILESAT 201	259.2	6637.337	500	6878.1370	6757.7369	0.0178166	5528.5507112	2764.2753556
2	The JCSAT-12	219.7	6597.8369	500	6878.1370	6737.987	0.0207999	5504.3320136	2752.1660068
3	The ARABSAT 5A	210.7	6588.837	500	6878.1370	6733.4869	0.0214821	5498.8187888	2749.4093944
4	The WILDBLUE-1	231.8	6609.937	500	6878.1370	6744.037	0.0198842	5511.7471398	2755.8735699
5	The W3B	213.2	6591.3369	500	6878.1370	6734.7369	0.0212925	5500.3500554	2750.1750277

TABLE 2. Delta-V and change of fuel mass for the five best-transferred satellites.

	Flights	Vp_1 (km/sec)	Vp_2 (km/sec)	ΔV_1 (km/sec)	Va_2 (km/sec)	Vf_2 (km/sec)	ΔV_2 (km/sec)	ΔV_{Total} (km/sec)	$\Delta m/m_1$
1	The NILESAT 201	7.81822802	10.1891178	2.3708898475	1.59889330	1.597935	-0.0009582775	2.369931569	0.4290
2	The JCSAT-12	7.85308024	10.2215245	2.3684442800	1.59946242	1.602633	0.00317064053	2.371614920	0.4293
3	The ARABSAT 5A	7.86106732	10.2294472	2.3683799147	1.59851867	1.602633	0.00411438673	2.372494301	0.4294
4	The WILDBLUE-1	7.84236909	10.2135307	2.3711616074	1.59505200	1.596949	0.00189748043	2.373059087	0.4295
5	The W3B	7.85884696	10.2293215	2.3704745898	1.59430345	1.598146	0.00384292184	2.374317511	0.4296

Our assessment of the orbit of the NILESAT 201 satellite revealed distinct variations between the theoretical model and the actual path with perturbations. The idealized trajectory, illustrated in Fig. 3(a), was established with the initial parameters: a semi-major axis of 6757.74 km, an inclination of 2°, an eccentricity of 0.0178166, a longitude of the ascending node at 0°, and an argument of perigee at 178°. This scenario assumes an undisturbed orbit, providing a controlled baseline for our analysis.

Upon introducing perturbative forces, as shown in Fig. 3(b), the satellite trajectory demonstrated notable deviations. We attribute these variations to several predominant forces: atmospheric drag, solar radiation pressure, gravitational influences from celestial bodies, and geomagnetic field interactions.

Specifically, the atmospheric drag exerted a substantial impact, inducing a quasi-linear decrease in the semi-major axis. This decay reflects progressive orbital degradation due to atmospheric resistance, which is particularly significant at the perigee where the atmospheric density is higher. Concurrently, there was a linear increment in the perigee's argument, suggesting a gradual shift in the orientation of the orbit.

In addition to drag, the orbit inclination underwent alterations that manifested as a combination of linear and secular trends. This pattern suggests an interplay between the direct atmospheric drag effects at lower altitudes and the more gradual, long-term influences of third-body gravitational interactions. The lunar

gravitational pull was evidenced by secular changes in both the longitude of the ascending node and the true anomaly, underscoring the Moon's proximity and its significant perturbative effect compared to the more distant Sun.

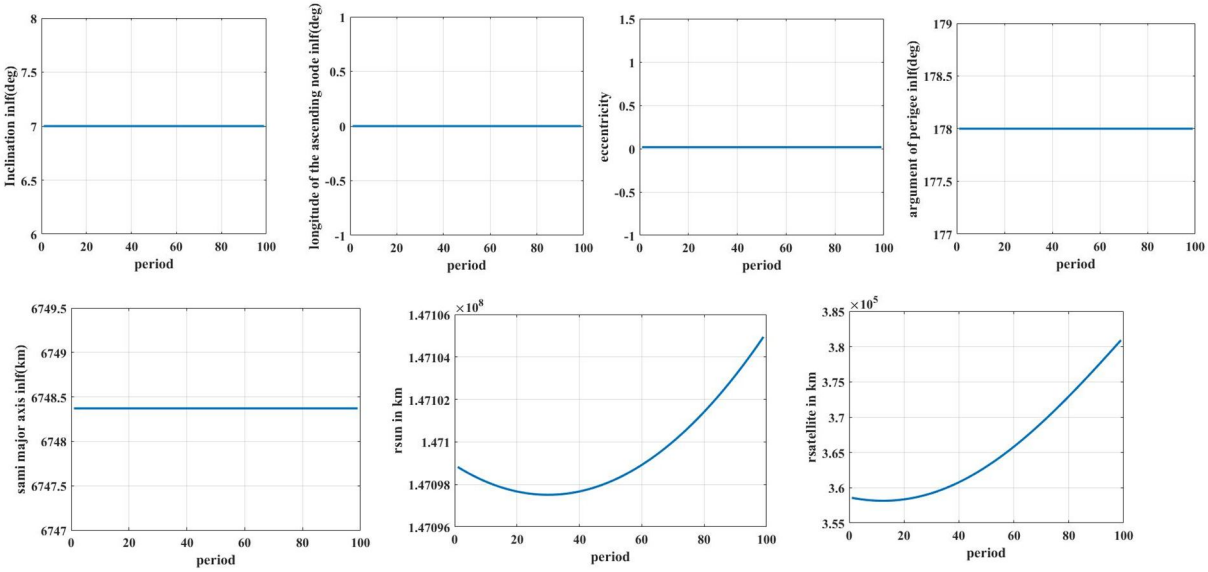

FIG. 3(a). Changes in orbital elements before the perturbation effects for the parking orbit of satellite NILESAT 201.

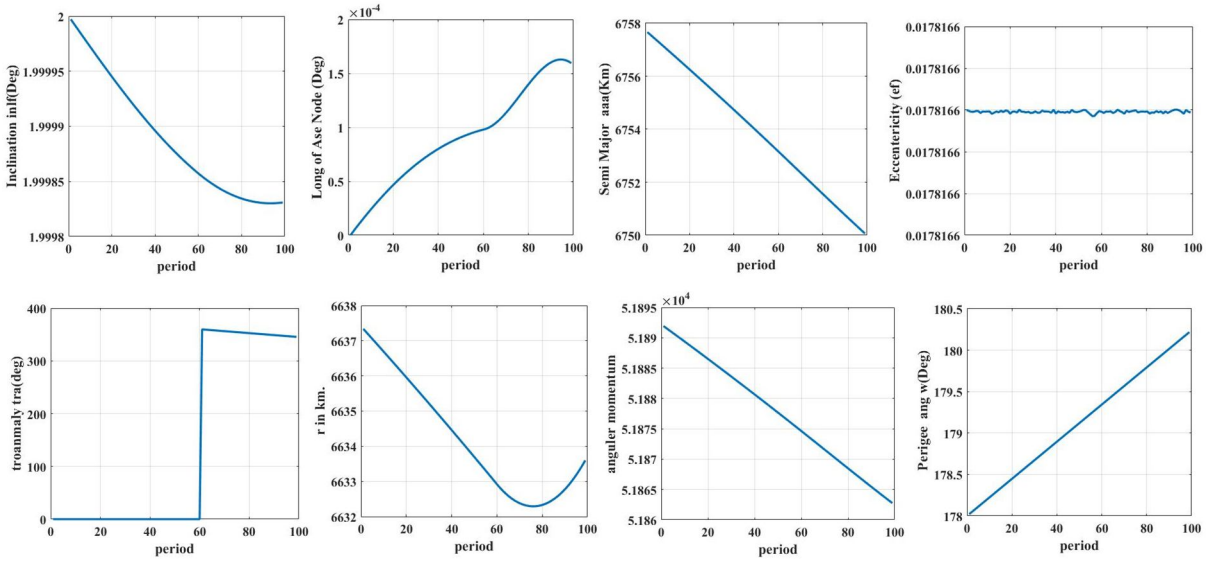

FIG. 3(b). Changes in orbital elements after perturbation effects for the parking orbit of satellite NILESAT 201.

Eccentricity remains largely consistent over time, which points to a minimal impact from orbital perturbations. This stability could be attributed to the satellite being located in a "sweet spot", where the gravitational influences of the Earth, Moon, and Sun largely cancel out, leading to a naturally stable orbit.

In summary, the perturbed orbit of NILESAT 201 presents a complex dynamical system that is influenced by a combination of deterministic and stochastic forces. Understanding these effects is paramount for effective station-keeping strategies, ensuring the longevity and reliability of the satellite's communication services. Future work will focus on quantifying the fuel budget for corrective maneuvers and optimizing the satellite's response to these perturbative forces.

The graphical representation of JCSAT-12's orbital parameters in Figs. 4(a) and 4(b) illustrates the stark contrast between an unperturbed orbit and on affected by various perturbative forces. In the ideal state shown in Fig. 4(a), the semi-major axis, inclination, eccentricity, longitude of the ascending node, and argument of perigee are presented with values of 6737.99 km, 2, 0.0207999, 0°, and 178°, respectively. These figures indicate a geostationary transfer orbit and are expected to

remain constant over time in the absence of external influences.

Under the perturbed conditions shown in Fig. 4(b), the trajectory of JCSAT-12 deviates from the ideal trajectory. The semi-major axis shows a decreasing trend, commonly associated with the atmospheric drag encountered by satellites at lower altitudes. The inclination exhibits both linear and secular behavior, suggesting the combined effects of atmospheric drag, which impacts the orbit immediately, and the more gradual influence of third-body attractions such as the gravitational pull of the Moon or Sun. The argument of the perigee's steady increase is typically linked to atmospheric drag effects, which are most pronounced at the orbit's closest approach to the Earth.

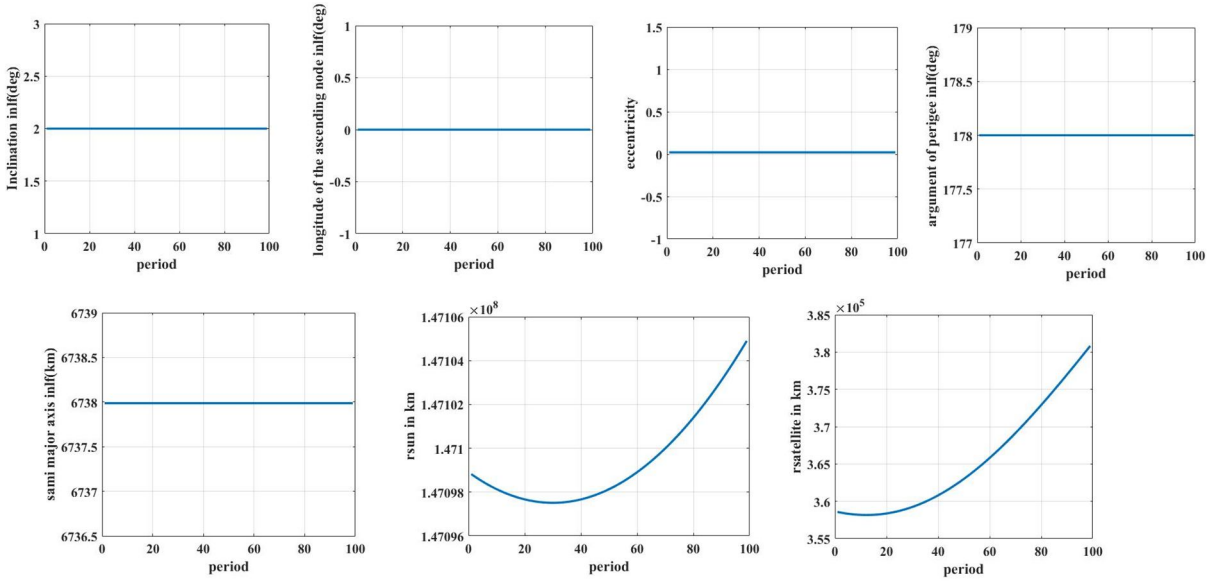

FIG. 4(a). Orbital elements' changes before the perturbations' effects for the parking orbit of satellite JCSAT-12

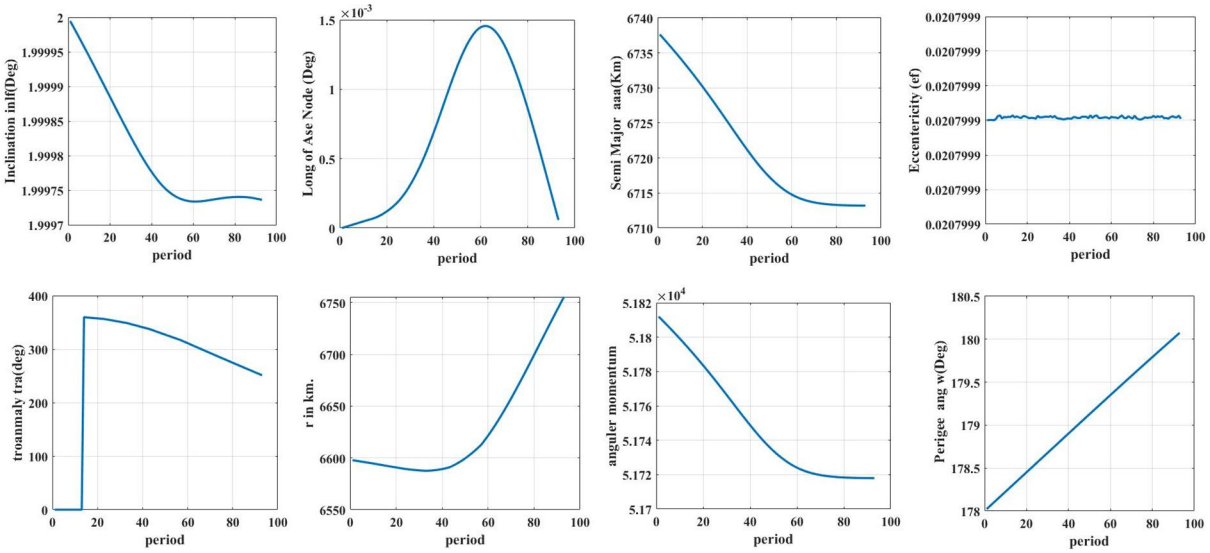

FIG. 4(b). Orbital elements' changes after the perturbations' effects for the parking orbit of satellite JCSAT-12.

Additionally, the longitude of the ascending node displays a mixture of secular drift and periodic variations. The secular drift can be attributed to Earth's oblateness, while the periodic component is likely due to the gravitational effects of the Moon and Sun, which are known to cause regression or progression of the node. Eccentricity exhibits remarkable consistency throughout the observed period, suggesting that the orbital perturbations have a negligible effect. The maintained stability implies a geostationary trajectory where disruptive forces may not significantly alter the orbit.

These variations in orbital parameters are critical for satellite operation because they

require precise station-keeping maneuvers to counteract these natural forces and maintain the satellite's desired geostationary orbit for reliable communication.

When examining the trajectory of the ARABSAT 5A satellite, we observed distinct behaviors under ideal and perturbed conditions. Fig. 5(a) outlines the initial, unperturbed orbit with the semi-major axis at 6733.49 km, inclination at 2 degrees, eccentricity at 0.0214821, right ascension of the ascending node at 0 degrees, and argument of perigee at 178 degrees. These values represent a controlled scenario without external perturbing influences, providing a reference for the designed path of the satellite.

According to Fig. 5(b), the introduction of perturbations significantly alters the trajectory of the satellite. The semi-major axis and inclination demonstrate not only a direct, linear response to atmospheric drag but also a secular trend over time, indicative of the sustained influence of third-body gravitational forces, such as those from the Moon and possibly the Sun. The argument of the perigee's linear increase further corroborates the impact of atmospheric drag, particularly at the point of the satellite's orbit closest to the Earth. The secular change in the true anomaly points to a steady alteration in the satellite's position within its orbit over time, primarily influenced by the gravitational pull of celestial bodies.

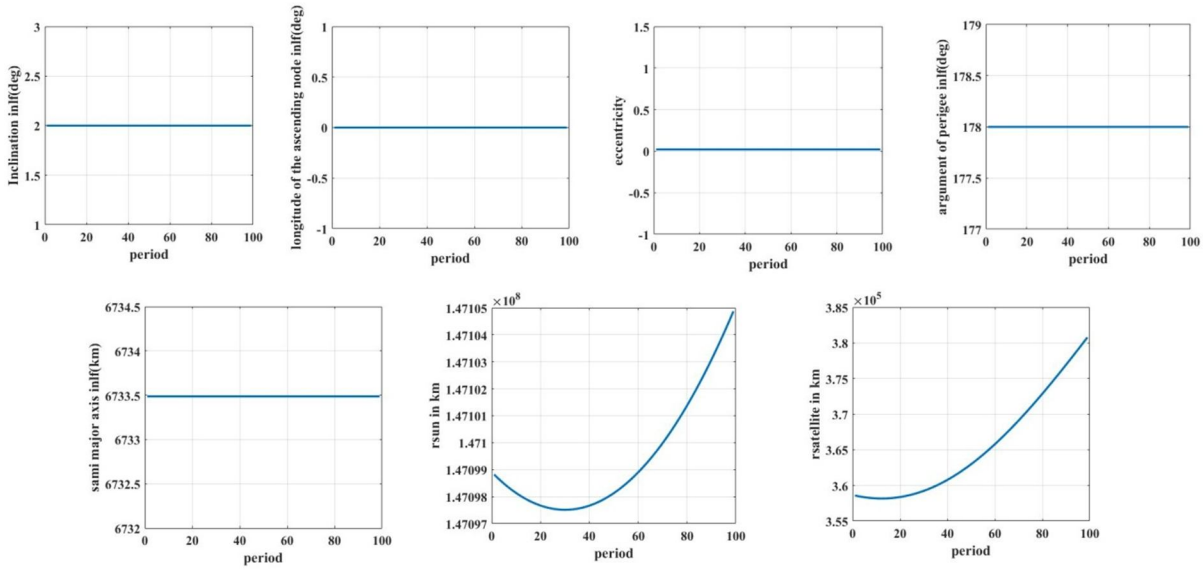

FIG. 5(a). Orbital elements' changes before the perturbations' effects for the parking orbit of satellite ARABSAT 5A.

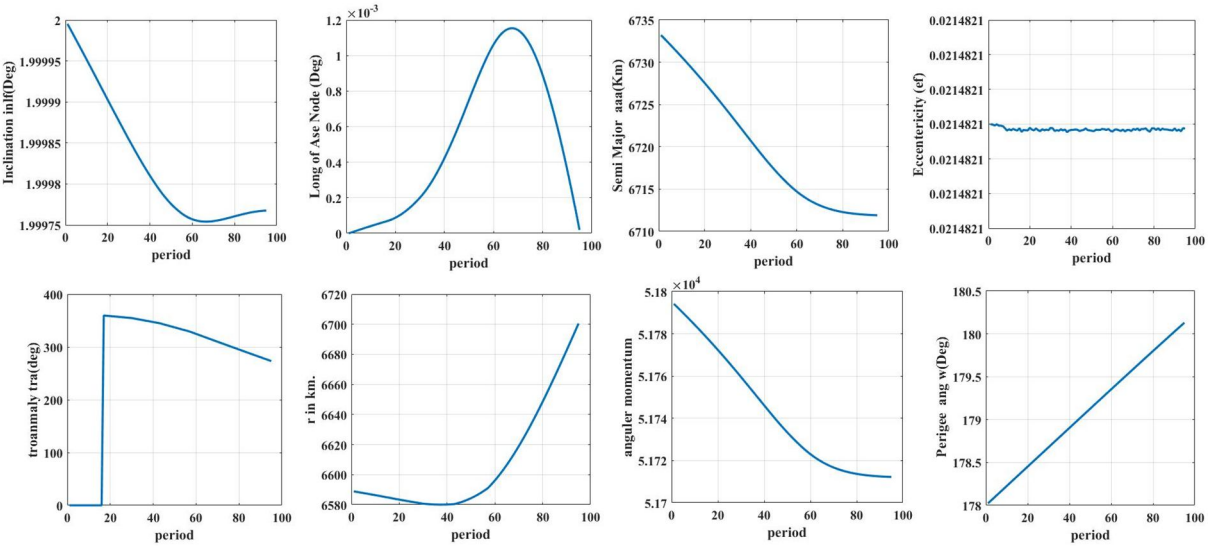

FIG. 5(b). Orbital elements' changes after the perturbations' effects for the parking orbit of satellite ARABSAT 5A.

Moreover, the right ascension of the ascending node's behavior reveals both secular drift and minor periodic fluctuations, a signature of the Earth's oblate shape affecting the orientation of the orbital plane. Finally, eccentricity demonstrates significant stability over time, indicating that the satellite's orbit is minimally affected by external perturbations. This consistent pattern suggests an equilibrium in the orbital path, where perturbative forces, such as atmospheric drag, Earth's non-uniform gravitational field, and third-body effects, do not substantially disrupt the satellite's trajectory.

These findings underscore the complex dynamical environment of orbital mechanics, necessitating continuous monitoring and adjustment to maintain ARABSAT 5A's intended orbit, ensuring its operational longevity and consistent delivery of satellite services.

The trajectory of the WILDBLUE-1 satellite, represented in Fig. 6(a), establishes a baseline for its orbital elements in an unperturbed state with a semi-major axis at 6744.04 km, inclination at 2°, eccentricity at 0.0198842, right ascension of the ascending node at 0°, and the argument of perigee at 178°. These values depict the expected path of the satellite in an idealized scenario, without the influence of external forces.

When we incorporate the dynamics of perturbations, the trajectory is significantly altered, as shown in Fig. 6(b). The forces at play include atmospheric drag, gravitational pull from third bodies such as the Moon and the Sun, and geopotential variations due to the Earth's non-spherical shape. Atmospheric drag is particularly impactful, reducing the velocity of the satellite and causing a decrease in the semi-major axis, which manifests as a secular decrease over time. This drag also influences the inclination, leading to a slow regression over time.

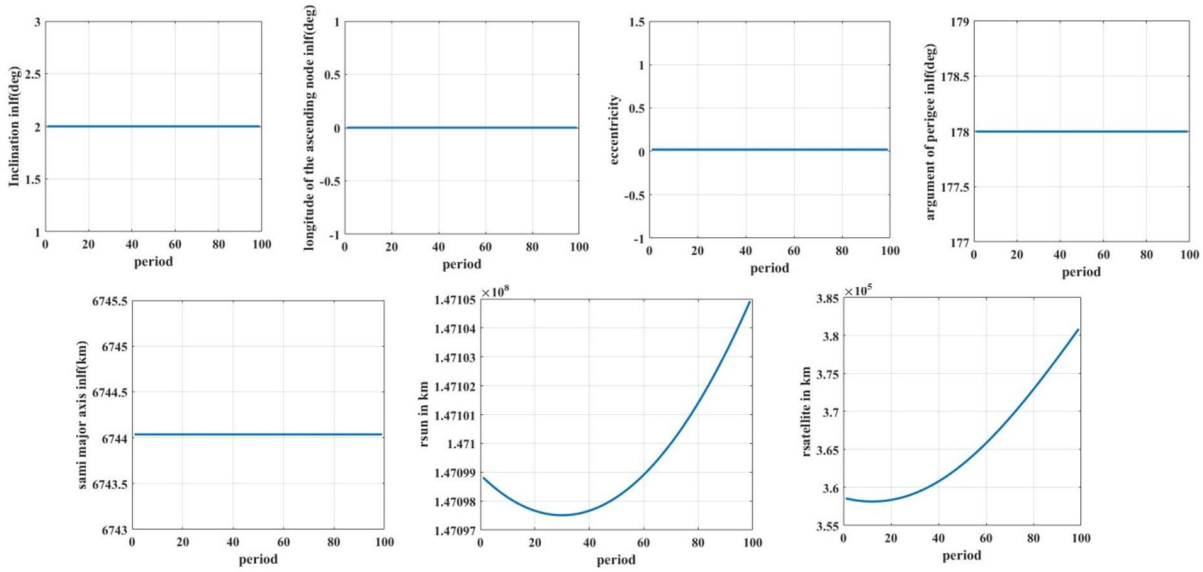

FIG. 6(a). Orbital elements' changes before the perturbations' effects for the parking orbit of satellite WILDBLUE-1.

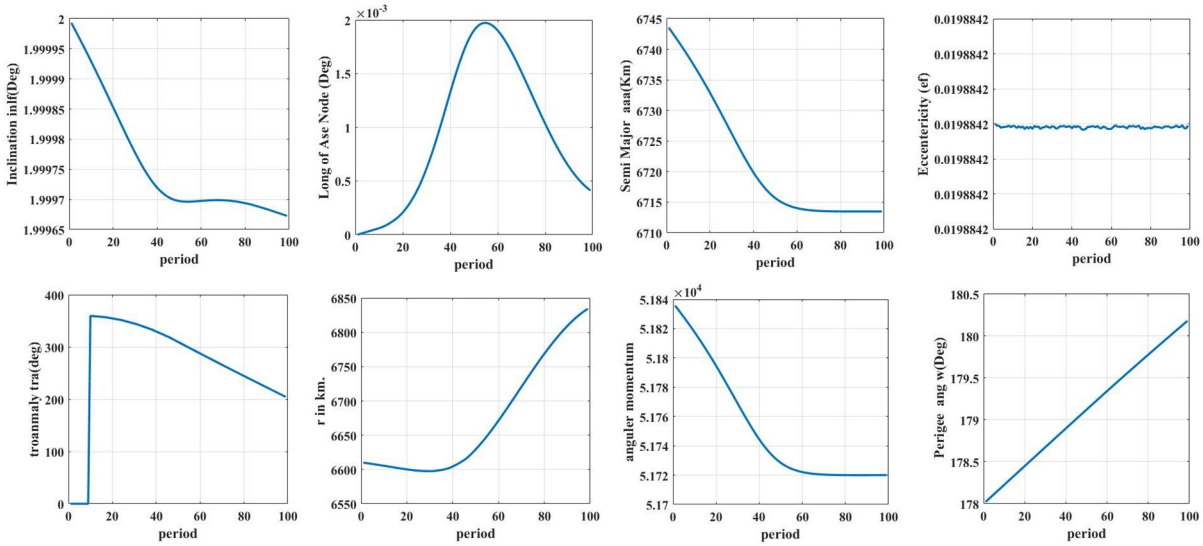

FIG. 6(b). Orbital elements' changes after the perturbations' effects for the parking orbit of satellite WILDBLUE-1.

The argument of perigee rises owing to atmospheric drag, indicating a gradual shift in the orientation of the orbit within its plane. This is a consequence of the differential drag experienced at various points in the orbit, especially at the perigee, where the atmosphere is denser. The periodic variation of the true anomaly, influenced by third-body attractions, shows that the Moon's gravitational pull alters the satellite's position within its orbit.

The longitude of the ascending node's behavior, with its mix of secular and periodic changes, signifies Earth's oblateness effect. This oblateness causes the precession of the orbital plane, which can be observed over an extended period. Eccentricity displays a persistent uniformity over the observed timeframe, implying that the influence of common orbital disturbances is limited. The steadiness of this orbital element suggests a resilient trajectory against perturbative forces.

In operational terms, these perturbations require regular orbital adjustments to maintain WILDBLUE-1's intended path for optimal service provision. The satellite controllers must constantly monitor these parameters and execute station-keeping maneuvers to counteract the perturbative effects, ensuring the longevity of the satellite and the continuity of its communication capabilities.

The figures for the W3B satellite present two distinct scenarios: an ideal trajectory without perturbations and one that includes the complex effects of various perturbative forces.

Figure 7(a) illustrates the initial, ideal state of W3B's orbit with parameters set at a semi-major axis of 6734.74 km, an inclination of 2°, an eccentricity of 0.0212925, a longitude of the ascending node at 0°, and an argument of perigee at 178°. These parameters define the expected orbit in a controlled environment without external influence.

Figure 7(b) depicts how this trajectory evolves under the influence of perturbations. Atmospheric drag, a result of the satellite's interaction with the Earth's atmosphere, impacts the satellite's motion, causing a decrease in both the altitude and semi-major axis over time. This effect is evidenced by the decreasing trend in the semi-major axis and is indicative of orbital decay common to satellites, particularly at lower altitudes where the atmosphere is denser.

The gravitational pull from other celestial bodies, specifically the Moon and Sun, introduces additional forces that alter the satellite's inclination and true anomaly. These changes manifest as secular variations in the orbit tilt and position, demonstrating the far-reaching influence of these third-body attractions.

Owing to its equatorial bulge and mass distribution, the non-spherical nature of the Earth's gravitational field exerts additional complexity on the motion of satellites. This uneven gravitational field leads to the precession of the orbit, as seen in the periodic and secular changes in the longitude of the ascending node and the argument of the perigee.

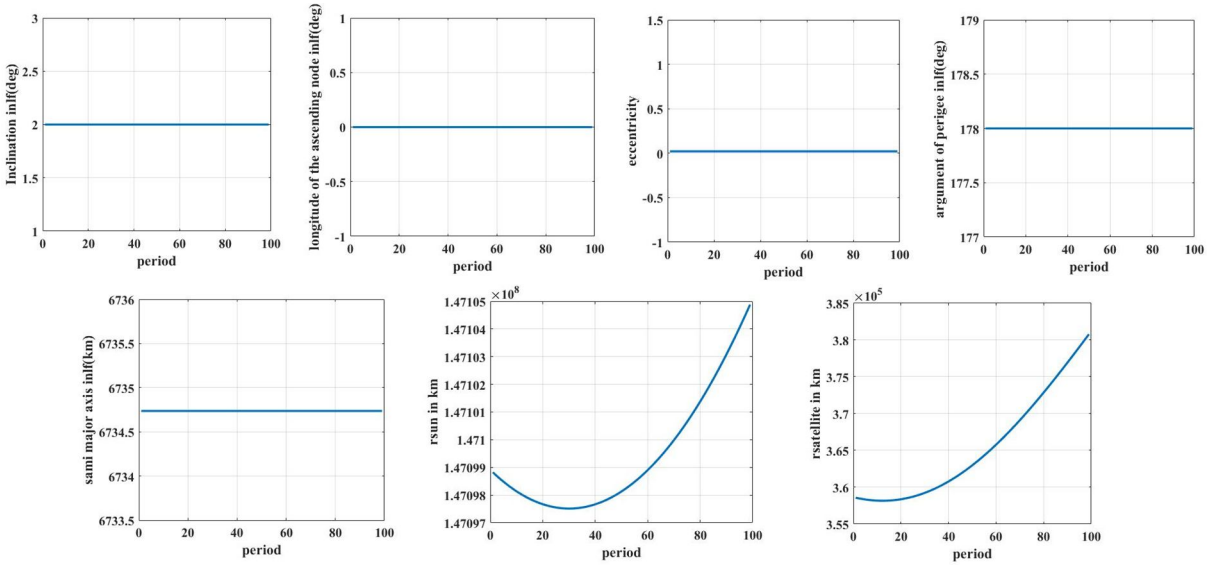

FIG. 7(a). Orbital elements' changes before the perturbations' effects for the parking orbit of satellite W3B.

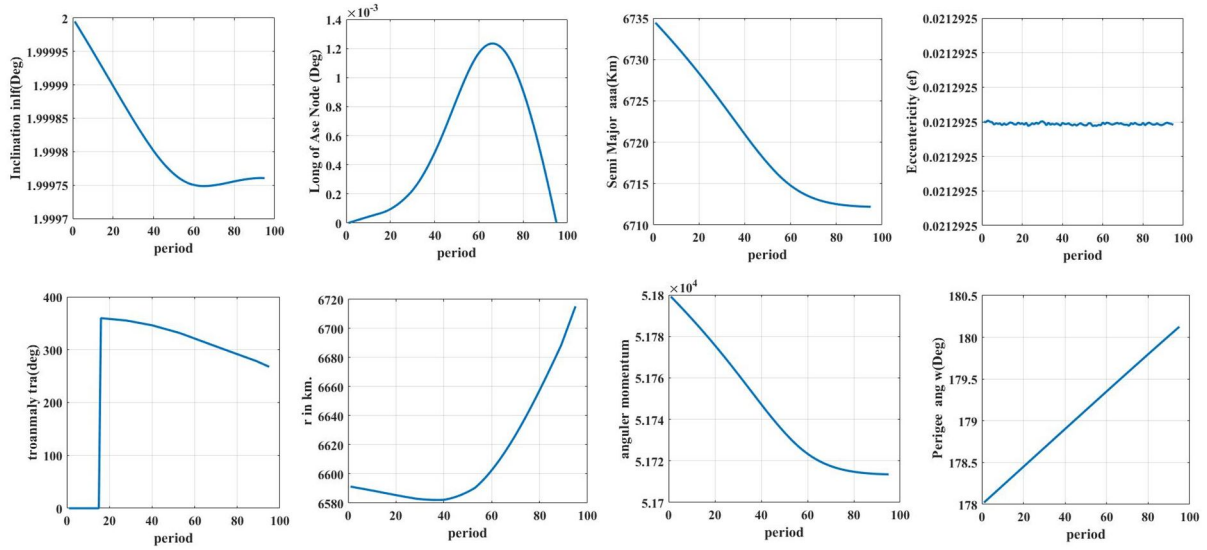

FIG. 7(b). Orbital elements' changes after perturbations' effects for the parking orbit of satellite W3B.

The perturbations did not influence eccentricity; the satellite maintained remarkable stability in this parameter, suggesting an orbit relatively unaffected by typical orbital disturbances.

This analysis underscores the need for continuous adjustment and control of the satellite's orbit. To counteract these perturbations and maintain the intended path of the satellite, regular station-keeping maneuvers are essential. These adjustments are crucial for the operational efficiency and reliability of satellite services.

Our study meticulously analyzed the propulsion and trajectory dynamics of five satellites: NILESAT 201, JCSAT-12, ARABSAT 5A, WILDBLUE-1, and W3B, as they transitioned from a low Earth orbit (LEO) to a geosynchronous transfer orbit (GTO) using the Hohmann transfer method. The efficacy of this technique was exemplified by the satellites' perigee and apogee heights, which were aligned with the desired calculated values, confirming their ability to maintain a stable position in the geosynchronous orbit. The high degree of agreement between our projections and actual outcomes emphasizes the pivotal role of precise transfer methods in conducting cost-effective satellite transport operations.

Perturbations, particularly atmospheric drag, have a significant influence on the trajectories of satellites, leading to a reduction in the semi-major axis and inclination, and signifying the impact on orbital decay. The gravitational pull from the Moon introduces additional complexity, causing periodic and secular changes in the

inclination and true anomalies of the satellites. Moreover, Earth's non-spherical gravitational field contributes to orbital precession, highlighting the intricacies of managing satellite trajectories.

The post-perturbation trajectory of each satellite, while commencing from comparable initial conditions, diverged owing to slight yet impactful differences in mass distribution, structural design, and size. This divergence necessitated a closer look at individual satellite responses, revealing nuanced reactions to varied perturbative forces.

In summary, the consolidated findings from our research deepen the understanding of satellite orbital mechanics, proving invaluable for precise crafting of satellite trajectories. This enhanced understanding is essential for mission planners to accurately steer satellites to their designated orbits, optimize their operational efficacy, and ensure the longevity of the service. Our study's insights equip mission designers with the foresight to anticipate and counteract perturbations, culminating in more dependable and successful satellite missions.

5. Conclusions

1. Efficiency of the Hohmann Transfer method: Our research confirms the Hohmann transfer method, which utilizes coaxial elliptical orbits, as a highly effective technique employed by Ariane 5 for satellite transfers. This method has demonstrated reliability in multiple satellite launches, reinforcing its value in space mission planning.
2. Optimization of parking orbit parameters: Through detailed analysis, we identified the optimal parameters for the parking orbit, which is a critical aspect of transitioning to the geosynchronous transfer orbit (GTO). Our findings suggest that initiating the transfer from an orbit altitude of 259.2 kilometers with a velocity of 7.81822802 kilometers/second, coupled with precise semi-major axis, eccentricity, inclination, argument of perigee, and longitude of ascending node values, is essential for efficient and accurate impulsive maneuvers into GTO.
3. Importance of revolutions in low orbit:

   For a successful impulsive maneuver into the GTO, it is essential that satellites complete a minimum of 50 revolutions in their parking orbit. This precondition is vital for achieving the desired orbital alignment and energy requirement for GTO insertion.
4. Perturbation analysis and management:

   Our comprehensive examination of various perturbations, including atmospheric drag, solar radiation pressure, gravitational effects, and magnetic field influences, sheds light on their impact on satellite trajectories. For satellites such as NILESAT 201, JCSAT-12, ARABSAT 5A, WILDBLUE-1, and W3B, these perturbations were significant but could be quantified and managed effectively. This management ensures the preservation of the trajectory integrity of these satellites.
5. Foundational research for future exploration: This study not only provides immediate insights into satellite dynamics and orbital transfers but also establishes a foundation for future research in this field. Understanding and managing the complex interplay between orbital perturbations is crucial for the advancement of satellite technology and strategic mission planning, particularly in the evolving landscape of space exploration.

Funding Statement

No funding was received for conducting this study. All research activities were performed without any financial support from external sources.

Conflict of Interest Declaration

The authors declare no conflicts of interest. This means they don't have any financial or personal connections that could unduly influence (bias) their work.

Author Contributions

All authors contributed equally to all aspects of the research and manuscript preparation.

Note: The flowchart presented in Appendix A provides a high-level overview of the computational model used in the code. Due to the complexity and detail of the calculations involved, detailed mathematical expressions and algorithmic steps are encapsulated within each block of the diagram. This approach is adopted to depict the overall structure and sequence of operations in the program while avoiding the intricacies of every mathematical expression or algorithmic step, which could be extensive and

complex. It's worth noting that these complex operations may require more than one sheet to explain in detail.

Appendix A. Flowchart of the Program for Orbital Parameter Calculations and Perturbation Analysis

The following flowchart illustrates the computational process used to calculate orbital parameters and analyze perturbations for satellites. The program begins with the initialization of the essential variables and the iterative calculations that account for various forces acting on the object. The process uses the Runge-Kutta integration method to solve the differential equations arising from these calculations. The flowchart delineates the sequence of operations from input parameters to the final output, ensuring a systematic approach to achieving accurate simulation results.

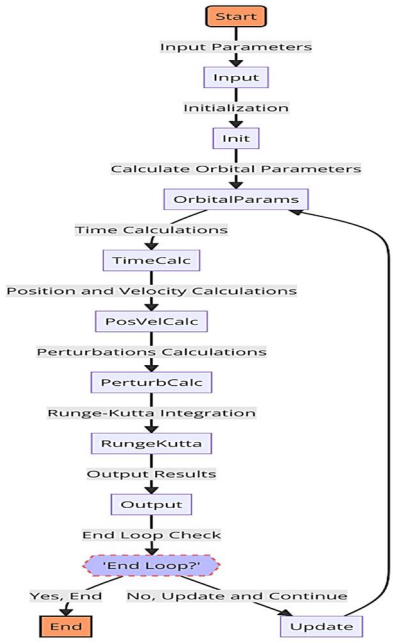

References

[1]"National Aeronautics and Space Administration (NASA)", [Online]. Available: https://www.nasa.gov.

[2] Ibraheem, A. and Salah, A., Iraqi J. Sci., 59 (4B) (2018) 2150.

[3]Vallado, D.A., "Fundamentals of Astrodynamics and Applications", (Springer Science & Business Media, 2001).

[4] Saleh, A. and Ghanem, H., Iraqi J. Sci., 54 (4) (2013) 1193.

[5] "Arianespace Official", [Online]. Available: https://www.arianespace.com.

[6] Hussien A., Jarad, M.M., and Mahdi, F.M., Iraqi J. Sci., 60 (4) (2019) 891.

[7] "International Telecommunication Union (ITU) publications on satellite communications", [Online]. Available: https://www.itu.int.

[8] Almohammadi, Mutlag, Iraqi J. Sci., 56 (2B) (2015) 1521.

[9] D. L. Mains, "Transfer Trajectories from Earth Parking Orbits", (Purdue University, 1993).

[10] Kim, J.L.S., Atmospheric Drag in Transfers between Geosynchronous Orbits, (2018).

[11] Yosif, M.A. and Saleh, A.-R.H., Iraqi J. Sci., 59 (1A) (2018) 199.

[12] Ibrahim, R.H. and Saleh, A.-R.H., Iraqi J. Sci., 60 (10) (2019) 2269.

[13] Mahdi, F.M., Salih, A.-R.H., and Jarad, M.M., Iraqi J. Sci., 61 (1) (2020) 224.

[14] Sharaf, M.A. and Sharaf, S.A.S., Rev. Mex. Astron. Astrofís., 52 (2) (2016) 283.

[15] Fadhil, O.A. and Saleh, A.-R.H., Iraqi J. Sci., 62 (2) (2021) 699.

[16] Yu, J., Yu, Y., Hao, D., Chen, X., and Liu, H., J. Aerosp. Eng., 233 (2) (2019) 686.

[17] Baron, A.S., "Orbital Mechanics and Astrodynamics: Techniques and Tools for Space Missions", Springer (2008).

[18] Wang, C., Guo, J., Zhao, Q., and Liu, J., Remote Sens., 10 (1) (2018) 118.

[19] Salih, M.J.F.A.R.H., Iraqi J. Sci., 57 (1B) (2016) 530.

[20] Al-Mohammadi, A.R.H.S., College of Science, University of Baghdad, Dec (2014).

[21] Yosif, M.A., and Saleh, A.-R.H., Iraqi J. Sci., 59 (1A) (2018) 199.

[22] Hale, F.J., "Introduction to Space Flight", 1st Ed. (1994).

[23] Ibrahim, R.H., "Improvement the Accuracy of State Vectors for the Perturbed Satellite Orbit Using Numerical Methods", University of Baghdad, College of Science, Department of Astronomy and Space, May 26, 2021.

[24] Cakaj, S.K.B. and Cakaj, A.E., Trans. Netw. Commun., (–) (–) 39.

[25] Al-Bermani, M.J.F. and Baron, A.S., J. Kufa Phys., 2 (1) (2010) 17–26.

[26] Saleh, A.-R.H., Iraqi J. Sci., 62 (2) (2021) 81.

[27] Singh, A.K.P.V.V.S.S., Adv. Space Res., 15 (3) (2018) 1170.

[28] Dos Santos, M.C., Department of Geodesy and Geomatics Engineering, University of New Brunswick, Canada, 1995.

[29] Al-Hiti, A.S.T., Master Thesis, Faculty of Science, University of Baghdad, 2002.

[30] Kaplan, E.D. and Kaplan, H.C., "Understanding GPS: Principles and Applications", 2nd Ed., Artech House, November 2005.

[31] Almohammadi, A.H.S. and Qahtan, A.Y., Iraqi J. Sci., 58 (3B) (2017) 1534.

[32] Leick, A., "GPS Satellite Surveying", 3rd Ed., Wiley, 2004.

[33]Mohammed, A., "Calculation of Perturbations Effect and Orbit Transfers for Earth Satellites", Ph.D. Thesis, University of Baghdad, 2019.

[34] Senga, D.P. and Senga, P., "Variation of Secondary Gamma Radiation Flux during Closest Approach of Mars towards Earth", Bhupal Nobles University, 2021.

[35]Yosif, M.A. and Saleh, A.-R.H., Sci.Int.(Lahore), 30 (5) (2018) 785.

[36]Hayder, R., "Computing the Perturbation Effects on Orbital Elements of the Moon", M.Sc. Thesis, University of Baghdad, 2011.

[37]Fortescue, S.J.G. and Fortescue, J., "Spacecraft Systems Engineering", 4th Ed., John Wiley & Sons, 2011.

[38] Saad, F.A. and Saleh, A.S.D.J., Iraqi J. Sci., 63 (12) (2022) 4090.

[39] Seeber, G., "Satellite Geodesy", 2nd Ed., revised, Walter de Gruyter, 2003.

[40] Liu, Y.L.Y.T.Z.D.X.Q.Y. and Liu, L.M., Remote Sens., 11 (24) (2019) 3024.

[41] Saleh, A.-R.H. and Damin, T.A., Iraqi J. Sci., 57 (1C) (2016) 775.

[42] Zainal, A.Q.I., Ph.D. Thesis, College of Science, University of Baghdad (2007).

[43] Wesam, W., Ph.D. Thesis, University of Baghdad (2011).

[44] Izzet, M.H.A.J.A.K.I., Iraqi J. Sci., 61 (2) (2020) 453.

[45] Fadhil, O.A., M.Sc. Thesis, Department of Astronomy and Space, College of Science, University of Baghdad, 2020.

[46] Battin, R.H., "An Introduction to the Mathematics and Methods of Astrodynamics", Rev. Ed., AIAA (1999).

[47] Crash, B., "Satellite Orbits: Models, Methods, and Applications", Springer, 2000.

[48] Montenbruck, O.G.E. and Gill, D.S., "Satellite Orbits: Models, Methods and Applications", 2nd Ed., Springer-Verlag Berlin Heidelberg, 2000..

[49] Markley, F.L. and Crassidis, J.L., "Fundamentals of Spacecraft Attitude Determination and Control", Springer, 1991.

[50] Broucke, R., Celest. Mech. Dyn. Astron., 25, 149–157, 1982.

[51] Izzet, A.K., Tikrit J. Pure Sci., 20(1), 142–149, 2015.

[52] Al-Bermani, M.J.F., Ali, A.H., Al-Hashmi, A.M., and Baron, A.S., J. Kufa Phys., 4(2), 1–6, 2012.